Main-Chain Chiral Smectic Liquid-Crystalline Ionomers Containing Sulfonic Acid Groups

Mei Tian, Bao-Yan Zhang, Fan-Bao Meng, Bao-Ling Zang

Centre for Molecular Science and Engineering, Northeastern University, Shen-yang 110004, People's Republic of China

Received 6 January 2005; accepted 22 April 2005
Published online in Wiley InterScience (www.interscience.wiley.com).
DOI 10.1002/app.22615

ABSTRACT: Three series of main-chain liquid-crystalline polymers (P1, P2, and P3) were synthesized by an interfacial condensation reaction of sebacoyl dichloride with various amount of brilliant yellow, isosorbide, and 4,4′-biphenydiol. P1 series are polyesters prepared from sebacoyl chloride and various amount of 4,4′-biphenyldiol and isosorbide. P2 series are polyesters prepared from sebacoyl chloride and various amount of 4,4′-biphenyldiol, brilliant yellow, and isosorbide. P3 series are polyesters prepared from sebacoyl chloride and various amount of 4,4′-biphenyldiol and brilliant yellow. P2 and P3 are main-chain liquid-crystalline ionomers. $P1_2$ and P3 series were prepared as model polymers for comparison with the liquid crystalline behavior of ionomers, P2 series. The structures of the polymers were characterized by IR and UV spectroscopy. Differential scanning calorimetry was used to measure the thermal properties of the polymers. The mesogenic properties were investigated by polarized optical microscope, differential scanning calorimetry, and X-ray diffraction measurements. The results show that P2 series are chiral smectic C ($S_mC^{*)}$ and chiral smectic B (S_mB^*) liquid crystalline ionomers exhibiting broken focal-conic texture and schlieren, as is the polymer $P1_2$, which has the same amount of 4,4′-biphenydiol and isosorbide. The introduction of ionic units in P2 series leads to an increase of clearing point, but has not affected the mesogenic type and texture, as compared with the corresponding polymer $P1_2$. The introduction of chiral units in P2 series leads to a change of mesophase, as compared with P3 series, which exhibit smectic C mesogetic phase. © 2005 Wiley Periodicals, Inc. J Appl Polym Sci 99: 1254-1263, 2006

Key words: main-chain liquid-crystalline ionomers (LCIs); chiral; isosorbide; sulfonate group; smectic

INTRODUCTION

In 1975, Meyer[1] presented theoretically and then proved experimentally that the chiral smectic mesophase was ferroelectric. A small molecule called HOBACPC, which was abistable, fast-switching electro-optical device, was demonstrated a few years later by Clark and Lagerwall.[2] Although a number of studies concerning low molecular weight chiral smectic liquid crystalline materials were previously reported, there have been only a few reports on polymeric chiral smectic liquid crystalline materials, especially on main-chain.[3] Therefore, it would be both necessary and useful to synthesize various kinds of liquid crystalline polymers (LCPs) to explore their potential applications.

LCPs show high strength and high stiffness properties. However, the major shortcoming that limits their application is the weak properties transverse to the fibre axis.[4] Moreover, in blends with other thermoplastic polymers, interfacial adhesion is weak. One approach to improving the transverse properties of LCPs and their adhesion with other polymers is to introduce ionic groups. Ionic groups should promote interchain interactions and improve the interfacial adhesion in the polymers,[5] especially for main-chain LCP containing ionic groups.[6–10] For example, thermotropic LCPs with ionic groups would offer the possibility for promoting intermolecular interaction through hydrogen bonds or ion-dipole association and improvement of the interfacial adhesion between the phases in blends.

In previous studies, we reported the synthesis of four main-chain thermotropic LCIs containing sulfonate groups. They are all nematic ionomers.[11–14] In this study, a new series of main-chain chiral smectic ionomers, P2 series, was prepared to show the effect of ionic groups on chiral smectic LCP, $P1_2$. In addition, a new series of main-chain smectic LCIs, P3 series, was prepared as model polymers for comparison with the liquid crystalline behavior of the ionomers, P2 series, to evaluate the effect of chiral building block on smectic LCIs, P3 series.

Correspondence to: B.Y. Zhang (baoyanzhang@hotmail.com)
Contract grant sponsors: National Natural Scientific Fundamental Committee, China, HI-Tech Research and development program (863), China, National Basic Research Priorities Program (973), China, Science and Technology Research Major Project of Ministry of Education of China, and Specialized Research Fund for the Doctoral Program of Higher Education

Journal of Applied Polymer Science, Vol. 99, 1254-1263 (2006)

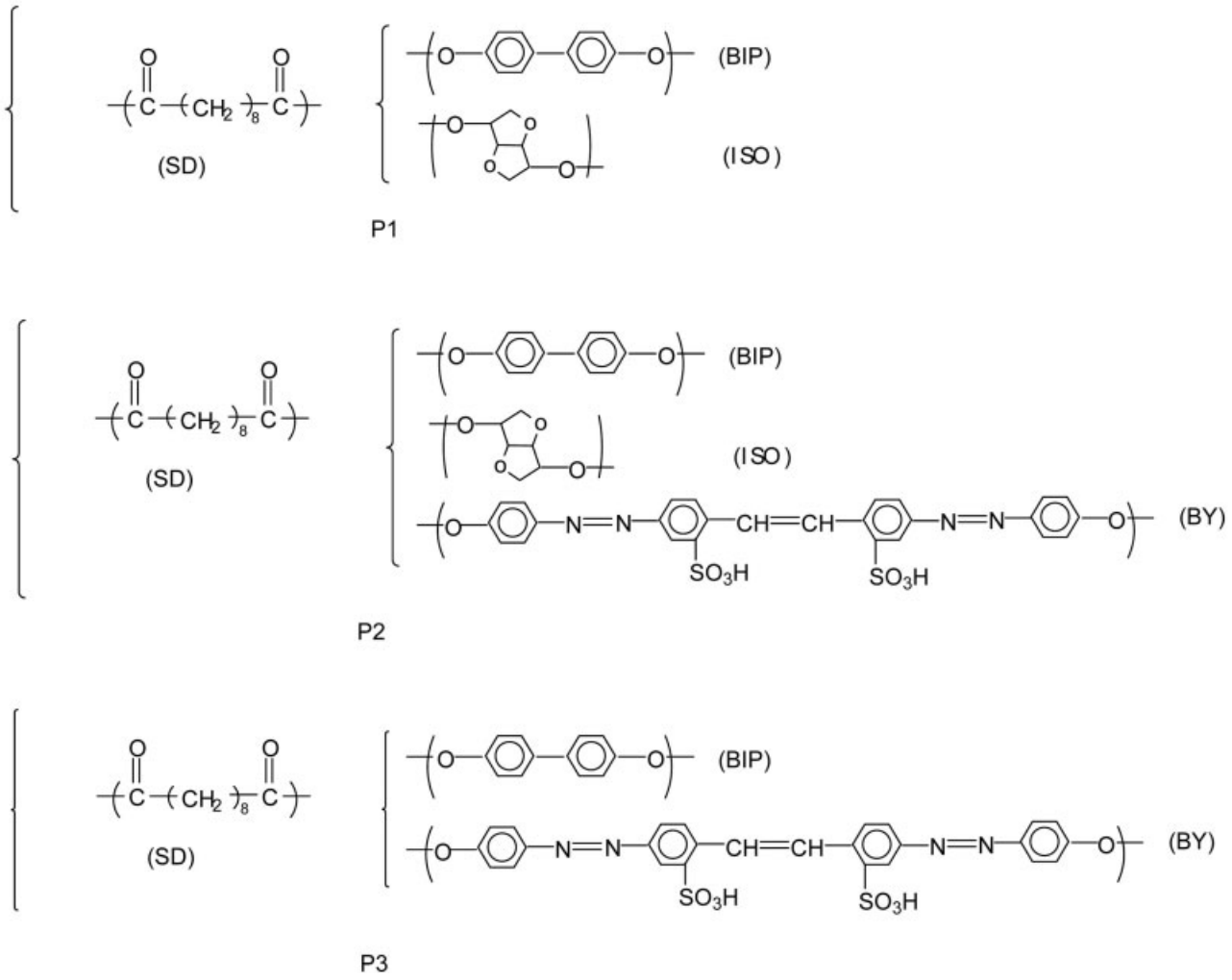

Scheme 1 The synthesis of polymers

EXPERIMENTAL

Materials

Brilliant yellow(BY, 98%), sebacic acid (SD 99%), 4,4′-Biphenyldiol(BIP, ≥99%) were obtained from Beijing Chemical Industry Company (China). Isosorbide(ISO, ≥98%) was bought from Yangzhou Shenzhou new material Co. (China). Thionyl chloride (bp, 78.8°C) and pyridine were obtained from Shenyang Chemical Industry Company (China). Pyridine was purified by distillation over KOH, before using. All solvents and reagents were used as received.

Characterization

IR spectra were measured using a Perkin–Elmer spectrum (Perkin–Elmer Instruments, Wellesley, MA), as KBr pellets. The UV spectra of solutions of the polymers P2 and P3 series in pyridine (c = 0.5 g/L) were measured with a Perkin–Elmer model 3840 UV-vis spectrometer equipped with a model 7500 data station (Perkin–Elmer Instruments, Wellesley, MA). Thermal transition temperatures were determined with a differential scanning calorimetry (DSC) 204 (Netzsch instruments) equipped with a liquid nitrogen cooling system at a heating and cooling rate of 10°C min^{-1} in a nitrogen atmosphere. The reported thermal transition temperatures were collected during the second heating cycle. A Leitz Microphot-FX (Leitz, Wetzlar, Germany) polarizing optical microscope (POM) equipped with a Mettler FP 82 hot stage and FP 80 central processor was used to observe phase transition temperature and analyze LC properties for the polymers through observation of optical textures. X-ray diffraction measurements were performed with nickel-filtered Cu-Kα(λ = 1.54 Å) radiation, using a Rigaku powder diffractrometer. The optical rotations were determined with a Perkin–Elmer Model 341 Polarimeter. Solutions of 2 g/L in pyridine were measured in 2-mL cuvettes of 100 mm length, using light of a Na-lamp at λ = 589 nm. Dilute solution viscosity measurements were carried out in pyridine solution at

TABLE 1
Polymerization, Specific Rotation, and Intrinsic Viscosity

Polymer	Feed (mmol)				ISO[a] (mol %)	BY[b] (mol %)	$[\alpha]_{589}^{30}$	$[\eta]^c$
	SD	BIP	ISO	BY				
$P1_0$	5.50	5.00	0	0	0	0	–[d]	0.560
$P1_1$	5.50	4.50	0.50	0	5	0	7.02	0.490
$P1_2$	5.50	4.00	1.00	0	10	0	28.6	0.451
$P1_3$	5.50	3.50	1.50	0	15	0	35.93	0.402
$P1_4$	5.50	3.00	2.00	0	20	0	38.18	0.371
$P1_5$	5.50	2.50	2.50	0	25	0	43.16	0.330
$P1_6$	5.50	2.00	3.00	0	30	0	57.29	0.305
$P2_1$	5.50	3.96	0.99	0.05	9.9	0.5	27.39	0.294
$P2_2$	5.50	3.92	0.98	0.10	9.8	1.0	26.54	0.287
$P2_3$	5.50	3.88	0.97	0.15	9.7	1.5	25.12	0.276
$P2_4$	5.50	3.84	0.96	0.20	9.6	2.0	25.80	0.275
$P2_5$	5.50	3.80	0.95	0.25	9.5	2.5	26.14	0.272
$P2_6$	5.50	3.76	0.94	0.30	9.4	3.0	26.26	0.263
$P3_1$	5.50	4.95	0	0.05	0	0.5	—	0.317
$P3_2$	5.50	4.90	0	0.10	0	1.0	—	0.208
$P3_3$	5.50	4.85	0	0.15	0	1.5	—	0.201
$P3_4$	5.50	4.80	0	0.20	0	2.0	—	0.192
$P3_5$	5.50	4.75	0	0.25	0	2.5	—	0.190
$P3_6$	5.50	4.70	0	0.30	0	3.0	—	0.184

[a] Mol % of ISO based on SD+BIP+ISO+BY.
[b] Mol % of B Y based on SD+BIP+ISO+BY.
[c] Intrinsic viscosity.
[d] No optical activity.

30 ± 0.2°C, using an Ubbelohde capillary viscometer. The flow times were kept sufficiently long, that is, >100 s, so that kinetic energy corrections could be neglected.

Synthesis of sebacoyl dichloride

Sebacic acid (0.1 mol) and thionyl chloride (0.3 mol) were placed in a 250-mL flask. The mixture was stirred for 2 h at room temperature, and then heated under reflux at 78°C for 4 h. The excess thionyl chloride was removed. The yield of SD is 85%. (bp, 168°C/12 mmHg).

Synthesis of polymers

The polymer synthesis is outlined in the Scheme 1, and the material compositions used in polymerization are summarized in Table I. For the synthesis of polymers P2 series, interfacial polymerizations were carried out in a high-speed warring blender. SD (5.5 mmol each) in dichloromethane (30 mL) was rapidly added to a slowly stirred aqueous layer (30 mL) composed of BIP, ISO, BY, 0.66 g of sodium hydroxide, and 0.133 g of butyltriethylammonium chloride. The polymers were recovered by slowly adding the resulting slurry to methanol (100 mL), stirring, and filtering. The polymers were washed repeatedly with fresh methanol and methanol/water mixture till the filtrate was clear and colorless, and finally dried in a vacuum oven at 50–60°C for at least 12 h.

IR (KBr) cm^{-1}: 3,366 (—OH), 2,920, 2,850 (—CH_2—), 1,737 (C═O), 1,601,1,496 (Ar), 1,200 (C—O—C).

RESULTS AND DISCUSSION

Polymerizations

The polymerization experiments are summarized in Table I. The polymer molecular weight is represented by the intrinsic viscosity measured in pyridine at 30°C. The relationship between M_v and the intrinsic viscosity,$[\eta] = kM^{\alpha}{}_v$, was referred to as Mark-Houwink equation. It does provide estimates for the molecular weights achieved for these polymers.

The intrinsic viscosity of P1 series decreased with the increasing content of ISO in the feed. The main reason may be the increase of flexibility of the chains in the polymers with increasing content of ISO in them.

The intrinsic viscosity of P2 and P3 series decreased with the increasing content of BY in the feed. The reason may be that once the BY reacted, the chain ceased to grow, that is, the addition of the hydrophilic BY pulls the growing chain into the aqueous phase and by doing so, removes the reactive end from the interface. As a result, the reactive end of the chain cannot react further with the acid chloride monomers

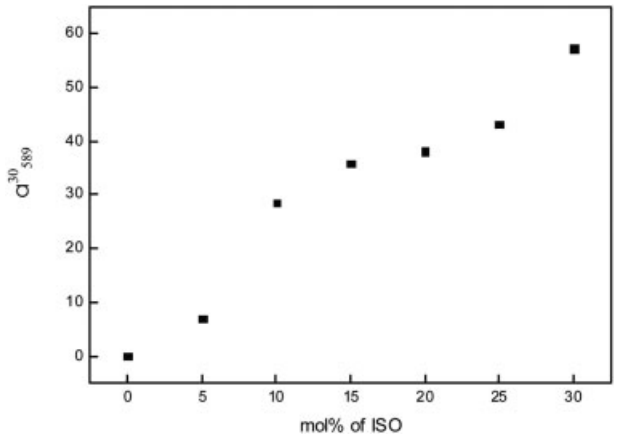

Figure 1 Variation of SROT with concentration of ISO in the polymers P1 series.

in the oil phase. Thus, the molecular weight and the intrinsic viscosity of P2 and P3 series decrease with the increasing content of BY in the feed.

Optical rotation

The isosorbide, the polymers $P1_1$–$P1_6$ and P2 series in pyridine solution are optically active in the light of a Na-lamp at $\lambda = 589$ nm. The specific rotation (SROT) of isosorbide is 60.5°, and the SROTs of the polymers $P1_1$–$P1_6$ and P2 series show similar positive values to isosorbide, as shown in Table I. The isosorbide SROT value was higher than that of the polymers. The variation of SROT for P1 series with the isosorbide content is shown in Figure 1. Figure 1 shows that the SROTs of P1 series increase depending on the increasing isosor-

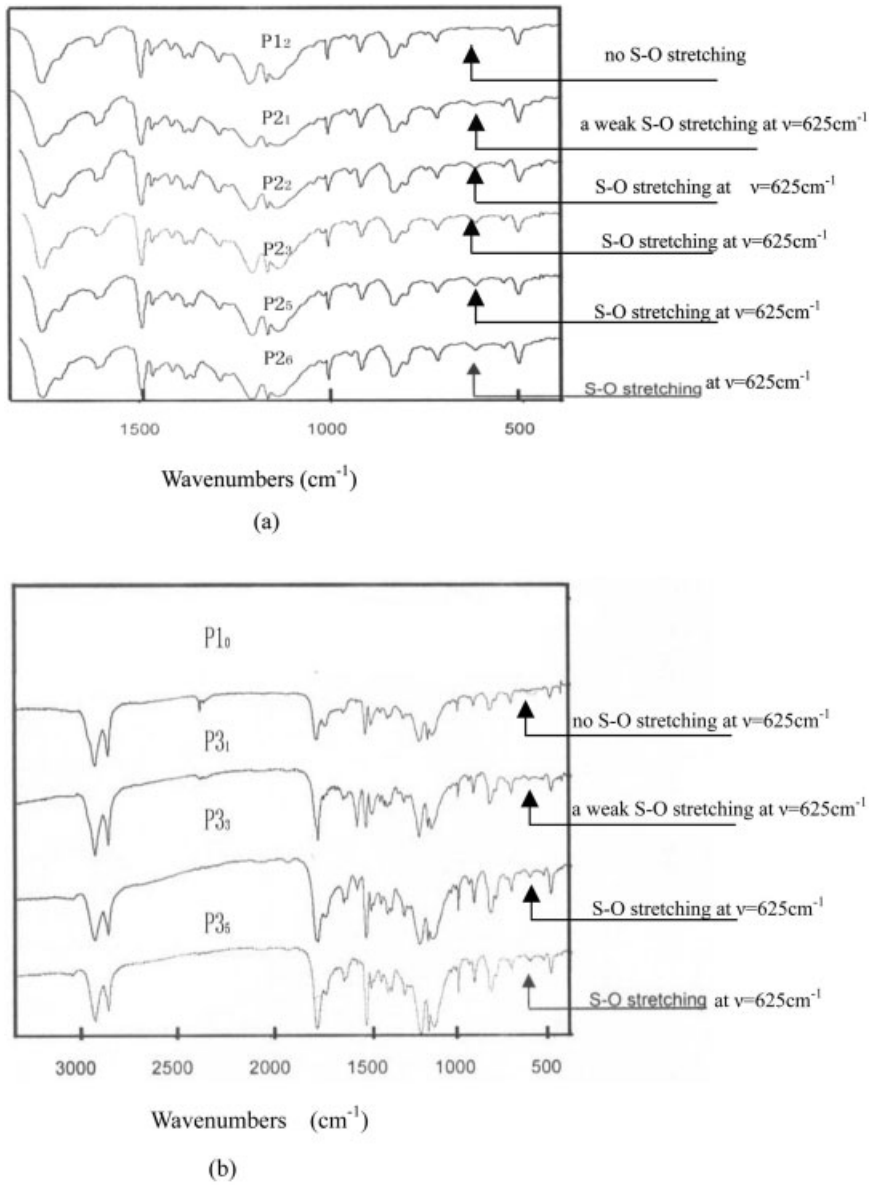

Figure 2 IR spectra for polymers.

bide content. The higher SROT of isosorbide and the increase of SROT of P1 series with increasing isosorbide content may be explained by the Van't Hoff optical rotation addition theory.[15] The SROT of an optically active compound is the total contribution of every chiral molecule. The concentration of optically active center per mass of polymer sample is lower than that of isosorbide alone; thus, the SROT of isosorbide is higher. The increase of SROT of P1 series is attributed to the increase in density of optically active centers per mass of polymer sample as the isosorbide increased in the polymerization reactions.

FTIR spectra

The characteristic absorption bands of the ionomers are mentioned above. For organic sulfonate, the FTIR absorption range of the O═S═O asymmetric and symmetric stretching modes lies in 1120–1230 cm^{-1} and 1010–1080 cm^{-1}, respectively, and that of the S—O stretching mode lies in 600–700 cm^{-1}. Because of the overlap found for both asymmetric and symmetric stretching bands of SO_2 with C—O in the polymers, the S—O stretching mode is chosen for identification of sulfonate groups in the ionomers. The difference between $P1_2$ and P2 series was that $P1_2$ did not contain BY groups, nevertheless P2 series contained them. Figure 2(a) compares the FTIR spectra in the range of 500–1500 cm^{-1} of $P1_2$ and P2 series, while there is no S—O stretching mode found in that of $P1_2$, and such modes as weak absorption bands are found at 625 cm^{-1} for the P2 series. These results clearly indicate successful incorporation of ionic groups in P2. The difference between $P1_0$ and P3 series was similar to that between $P1_2$ and P2 series, namely $P1_0$ did not contain BY groups, nevertheless P3 series contained them. Figure 2(b) compares the FTIR spectra in the range of 500–3000 cm^{-1} of $P1_0$ and P3 series, while there is no S—O stretching mode found in that of $P1_0$, and such modes as weak absorption bands are found at 625 cm^{-1} for the P3 series. These results clearly indicate successful incorporation of ionic groups in P3.

UV spectroscopy

The UV absorption spectra of $P1_2$, P2 series and $P1_0$, P3 series in the region λ = 300–600 nm are shown in Figures 3(a) and 3(b), respectively. The absorption peak at λ = 400 nm was due to the BY in the LCIs. The absorbance intensity of the peak increased with an increasing BY concentration in the feed. The result of UV analysis showed that the amount of BY in the LCIs increased with the increasing amount of BY in the feed. We are sure that the increase of the absorbance intensity of the peak (λ = 400 nm) was not due to the BY monomer because BY monomer is soluble in the water, and the polymers were washed repeatedly with fresh methanol and methanol/water mixture until the filtrate was clear and colorless, which showed BY monomer was washed away. For the reason, we are sure that the increase of the absorbance intensity of the peak (λ = 400 nm) was due to the increase of BY concentration in the polymers. The UV result indicated not only successful incorporation of BY groups, but also an increasing amount of BY in the polymers with increasing amount of BY in the feed.

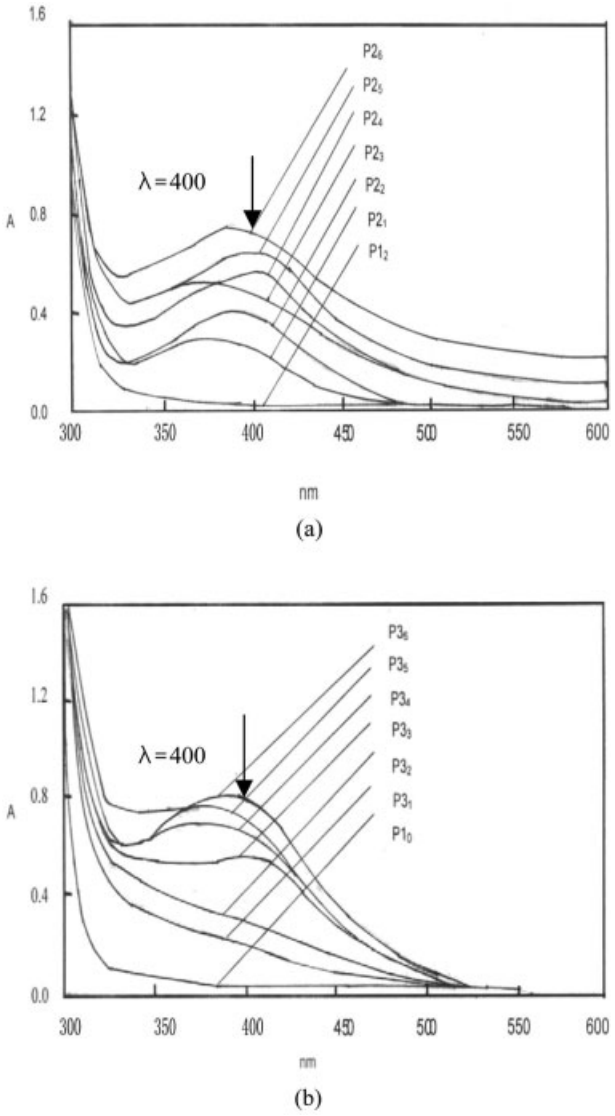

Figure 3 Effect of the BY content on the UV absorption of polymers (C = 0.5 g/L).

Thermal analysis

The phase-transition temperatures and corresponding enthalpy changes of P1, P2, and P3 series obtained on the second heating are summarized in Table II. Rep-

TABLE 2
DSC and POM Results of Polymers

	Cr_1–Cr_2		Cr-LC_1		LC_1–LC_2		LC_2-I			
Polymer	T[a] (°C)	T_g[b] (°C)	T_m[c] (°C)	ΔH_m (J g^{-1})	T_1[d] (°C)	ΔH_1 (J g^{-1})	T_i[e] (°C)	ΔH_i (J g^{-1})	ΔT[f] (°C)	LC Phase
$P1_0$	67.0	167.0	202.0	7.04	—	—	222.6	0.14	20.6	S_mC
$P1_1$	64.8	123.9	159.6	9.14	195.0	3.10	213.0	0.40	53.4	S_mB^*, S_mC^*
$P1_2$	63.4	111.2	141.0	4.71	160.9	2.25	186.8	0.25	45.8	S_mB^*,S_mC^*
$P1_3$	61.0	110.0	140.2	3.14	151.8	0.80	175.1	0.66	34.9	S_mB^*,S_mC^*
$P1_4$	60.9	108.0	138.6	3.59	149.5	0.53	171.0	0.14	32.4	S_mB^*,S_mC^*
$P1_5$	60.6	105.0	137.4	3.37	145.1	0.37	163.8	0.58	26.4	S_mB^*,S_mC^*
$P1_6$	60.4	104.0	131.0	3.12	139.0	0.52	158.0	0.52	27.0	S_mB^*,S_mC^*
$P2_1$	66.0	130.9	159.9	1.53	179.7	0.51	216.1	0.61	56.2	S_mB^*,S_mC^*
$P2_2$	64.6	130.6	156.0	2.50	178.3	0.49	211.0	0.28	55.0	S_mB^*,S_mC^*
$P2_3$	65.0	130.2	155.6	1.65	176.6	0.33	207.0	0.33	51.4	S_mB^*,S_mC^*
$P2_4$	64.0	129.8	154.5	1.36	175.1	0.90	204.5	0.47	50.0	S_mB^*,S_mC^*
$P2_5$	63.5	129.2	154.0	1.05	174.0	0.98	203.5	0.98	49.5	S_mB^*,S_mC^*
$P2_6$	61.8	128.8	152.8	0.70	173.2	0.78	201.1	0.25	48.3	S_mB^*,S_mC^*
$P3_1$	68.4	136.1	164.5	3.62	—	—	242.0	0.60	77.5	S_mC
$P3_2$	65.6	135.0	163.7	3.61	—	—	226.0	0.33	62.3	S_mC
$P3_3$	60.3	134.6	162.6	5.25	—	—	211.0	0.32	48.4	S_mC
$P3_4$	57.4	134.2	162.0	6.30	—		199.0	0.89	37.0	S_mC
$P3_5$	56.7	133.4	159.0	3.76	—	—	190.0	0.41	31.0	S_mC
$P3_6$	56.4	132.6	151.0	2.52	—	—	184.0	0.35	33.0	S_mC

[a] Transition temperature from crystal 1 to crystal 2.
[b] The glass transition temperature.
[c] The melting temperature.
[d] Transition temperature from S_mB^* to S_mC^*.
[e] The clearing point.
[f] Mesophase temperature ranges (T_i–T_m).

resentative DSC curves of the polymers are presented in Figure 4.

For P1, P2, and P3 series, an enthalpy change was observed at about 60°C. This is the transition temperature from crystal 1 to crystal 2.

The glass-transition temperature (T_g) is an important parameter in connection with structures and properties of polymers. In general, the factors of chain flexibility, molecular weight, and interchain interactions will affect the T_g. The results of the thermal analysis showed that T_g of the polymers P1 series decreased with an increase of the concentration of isosorbide in them. As we know, T_g decreases with an increase of the mobility of chain segments. For polymer P1 series, with an increase of the concentration of isosorbide, the concentration of 4,4′-biphenyldiol decreased, which made the chain flexibility increase, and thus the mobility of chain segments increased and the T_g decreased.

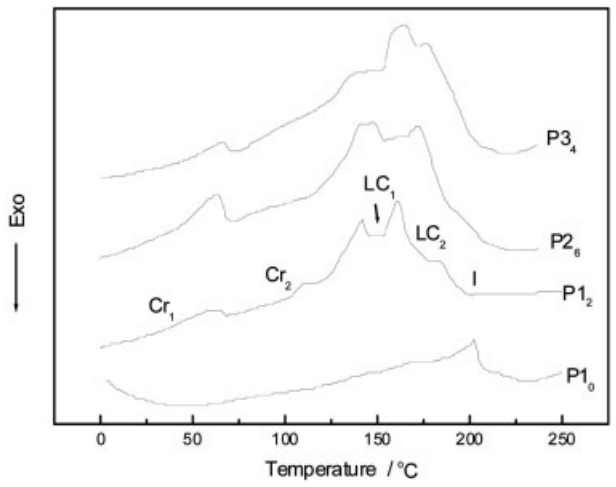

Figure 4 DSC thermograms (second heating) of polymers.

Table II shows that the T_g of P2 and P3 series decreased with an increase in BY concentration. A common observation in ionomers is that T_g increases with an increasing salt group concentration,[16] which attributes to intermolecular ionic interactions. The other observation is that T_g decreases with an increasing pendant concentration in the polymers, which is due to the large free-volume occupied by the polymer chains. In this study, both of the effects affected the T_g of P2 series, but neither of them predominated; therefore, the T_g decreased slightly from $P2_1$ to $P2_6$ and this is the same reason for the decrease of T_g of P3 series.

The melting temperature (T_m) of P1 series decreases with an increasing isosorbide concentration, which may be due to the increase of the flexibility of the chains in them.

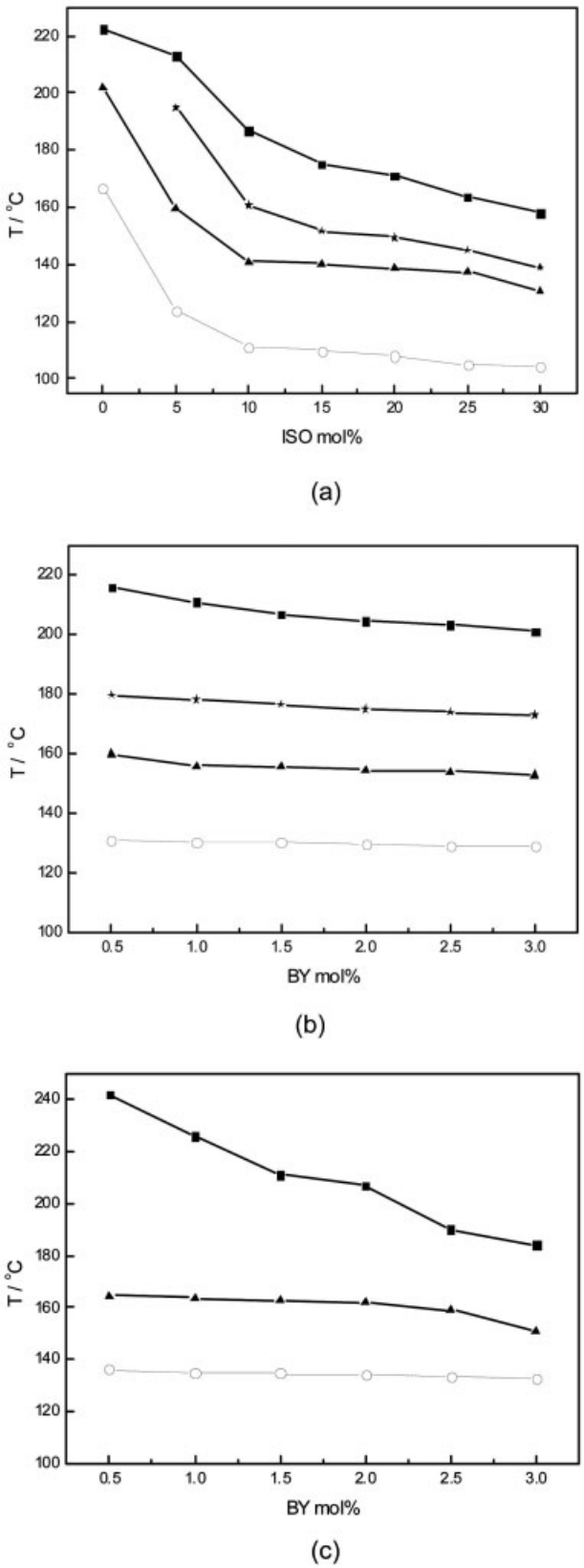

Figure 5 Effect of ISO or BY content on phase transition temperatures of the polymers. (a) effect of ISO content on phase transition temperatures of P1 series. ■ T_i, ★T_1, ▲T_m, ○T_g. (b) effect of BY content on phase transition temperatures of P2 series. ■ T_i, ★T_1, ▲T_m, ○T_g. (c) effect of BY content on phase transition temperatures of P3 series. ■ T_i, ▲T_m, ○T_g.

Table II shows that the T_m of $P2_1$ is higher than that of $P1_2$. The reason may be due to $P2_1$ containing BY groups and the concentration of the BY is low, thus the effect of intermolecular ionic interaction dominated and made the T_m of $P2_1$ increase. With the increasing of the concentration of BY in P2 series, the effect of large free volume of the pendant groups increased gradually, which could make T_m decrease, and the both factors have affected the melting temperatures, but neither of them dominated. Thus the melting temperature of P2 series decreased slightly with the increase in the concentration of BY in them. On the other hand, the decrease of the melting temperature of P2 series may be due in part to the decrease in molecular weight. This is demonstrated by the decrease of the intrinsic viscosity of P2 series, shown in the Table I.

The melting temperature of P3 series decreased with the increase in the concentration of BY in them and this may be due to the same reason as that for P2 series.

P11–P16 and P2 series have a LC phase-transition temperature T_1 (LC1–LC2), which has been identified by POM result and X-ray result.

Clearing point (T_i) is influenced by the flexibility of the chain, the regularity of polymer molecule, and the steric effect of large groups. The T_i of P1 series decreased with increasing the concentration of isosorbide. This may be due to the increase of flexibility of the chain in the polymers, which would reduce the energy of disorientation of polymer molecules in the LC phase.

The T_i of P2 decrease with increasing the concentration of BY in them, which may be partly due to the decrease of molecular weight (which is identified by the decrease of the intrinsic viscosity of P2 series, shown in the Table I) and partly to the large free-volume occupied by the BY groups (which would destroy the regularity of the chains of polymer molecules and reduce the energy of disorientation of polymer molecules in the LC phase).

The T_i of P3 decrease with the increasing concentration of BY in them and this may be due to the same reason as that for P2.

The T_i of $P2_1$ is higher than that of $P1_2$. As we know, owing to the introduction of ionic groups, the intermolecular ionic interaction will increase the T_i of polymer, and the large free volume of BY will destroy the regularity resulting in the decrease of T_i of the polymer. In this condition, the former may be superior to the latter, due to $P2_1$ containing a low concentration of BY.

The effect of ISO content on phase transition temperatures of P1 series is shown in Figure 5(a), and the effect of BY content on phase transition temperatures of P2 series and P3 series is shown in Figures 5(b) and 5(c), respectively.

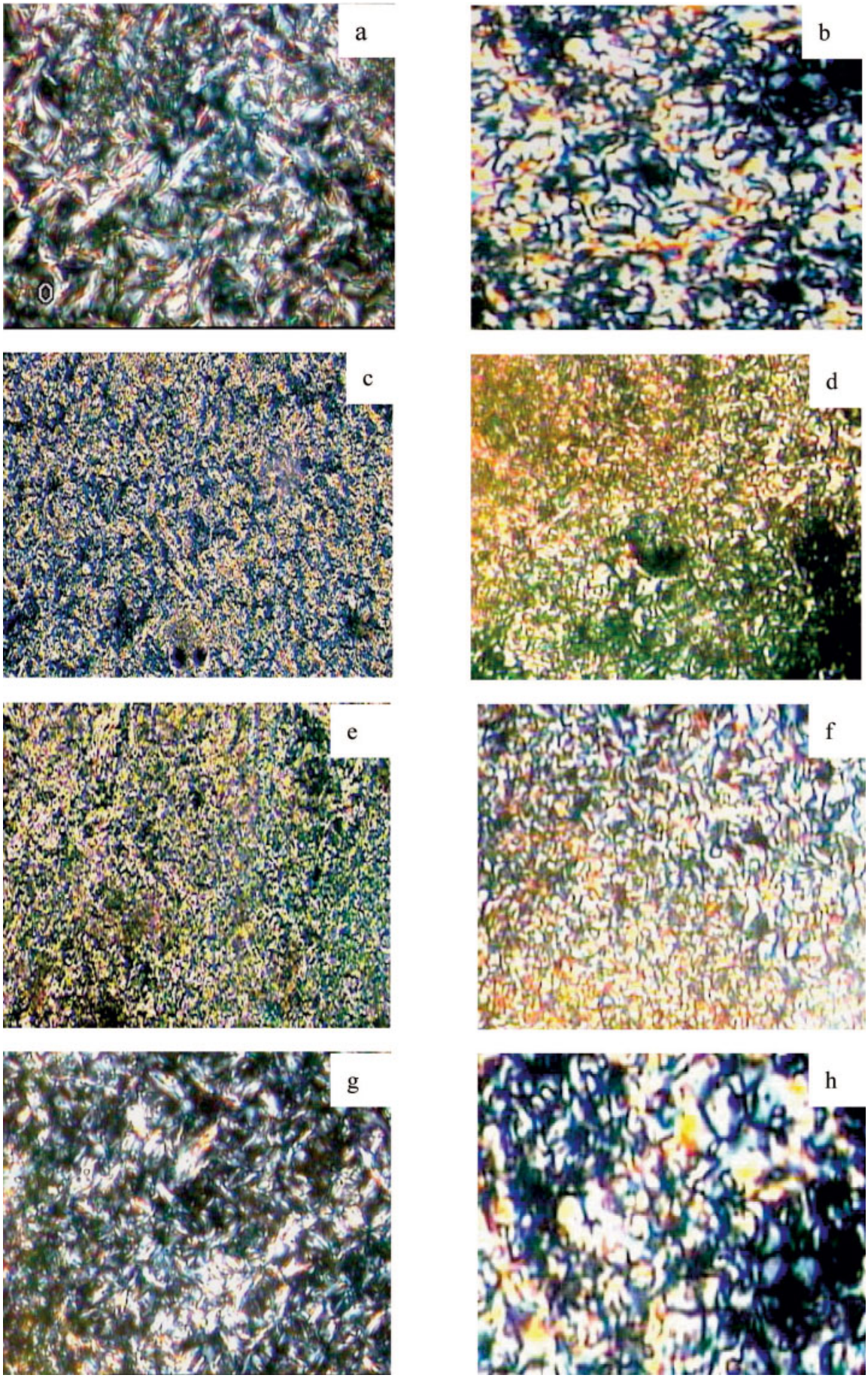

Figure 6 Polarizing optical micrographs (×200) of polymers: (a)Broken fan-shaped texture of the S_mC of $P1_0$ on cooling to 212°C;(b) Schlieren texture of the S_mC of $P1_0$ on heating to 206°C; (c) Broken fan-shaped texture of the S_mB^* of $P1_4$ on heating to 145°C; (d) Schlieren texture of the S_mC^* of $P1_5$ on cooling to 154°C; (e) Broken fan-shaped texture of the S_mB^* of $P2_1$ on heating to 175°C; (f) Schlieren texture of the S_mC^* of $P2_1$ on heating to 190°C; (g) Broken fan-shaped texture of the S_mC of $P3_1$ on cooling to 213.7°C; and (h) Schlieren texture of the S_mC of $P3_1$ on heating to 208°C. [Color figure can be viewed in the online issue, which is available at www.interscience.wiley.com]

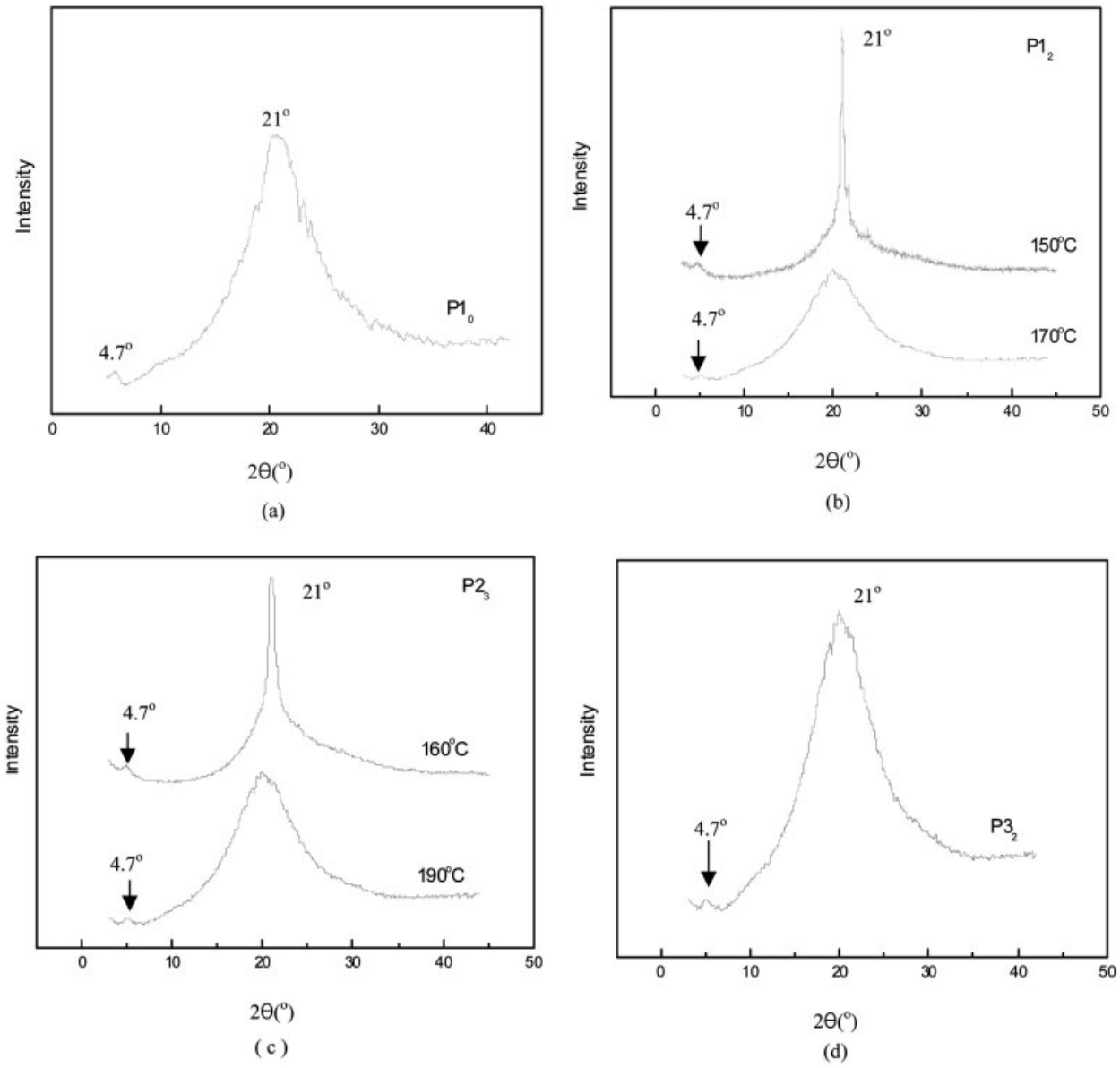

Figure 7 X-ray patterns of the quenched polymers.(a) $P1_0$ was quenched at 210°C;(b) $P1_2$ was quenched at 150 and 170°C, respectively; (c) $P2_3$ was quenched at 160 and 190°C, respectively; and (d) $P3_2$ was quenched at 190°C.

Textures analysis

All the polymers displayed a thermotropic mesophase and exhibited different colorful textures when observed under POM. The $P1_0$ exhibited clear schlieren texture and broken fan-shaped texture on heating and cooling cycles. When $P1_0$ was heated to 202°C, the sample began to melt, the typical schlieren texture gradually appeared, and the texture disappeared at 223°C. When the isotropic state was cooled to 218°C, the broken fan-shaped texture appeared, and then transformed into schlieren texture, which did not disappeared till room temperature. Photomicrographs of $P1_0$ are shown in Figure 6(a,b).

$P1_1$–$P1_6$ exhibited the broken fan-shaped and schlieren texture on heating and cooling cycles, as shown in Figure 6(c,d). P2 series displayed the broken fan-shaped texture and schlieren texture on heating and cooling cycles, as shown in Figure 6(e,f). P3 series exhibited clear schlieren texture and broken fan-shaped texture on heating and cooling cycles, as shown in Figure 6(g,h).

X-ray diffraction analysis

XRD studies were carried out to obtain more detailed information on the LC phase structure and type. Representative XRD curves of quenched samples are shown in Figure 7. A diffuse peak at about $2\theta = 21^{\circ}$ in WAXD curves and a weak small-angle reflection at about $2\theta = 4.7°$, which correspond to a d-spacing of d

= 18.8 and 4.2 Å, were observed for $P1_0$, which is shown in Figure 7(a). This was in correspondence with the result of the textures of $P1_0$, which indicated $P1_0$ is S_mC phase. For $P1_1$–$P1_6$ and P2 series quenched between the T_m and the T_1(the transition temperature from LC_1 to LC_2), a weak small-angle reflection associated with the smectic layers and a strong sharp peak associated with lateral packing were observed at about $2\theta = 4.7$ and 21°, as shown in Figure 7(b,c). However, when quenched between the T_1 and the T_i, a diffuse peak at about $2\theta = 21°$ and a weak small-angle reflection at about $2\theta = 4.7°$ were observed, as shown in Figure 7(b,c). Generally, in LC main-chain polymers sharp reflections at small angles and reflections at wide angles arising from the ordered smectic phase are observed in the solid state (solid mesophase).[17] The sharp peak at about $2\theta = 21^\circ$ reflected that the polymers had highly ordered smectic phase. The result of X-ray diffraction analysis, POM, and optical rotation of the $P1_1$–$P1_6$ and P2 series indicated that they can exhibit S_mB^* and S_mC^* mesophase at different temperature. The results also indicated that the introduction of ionic groups in P2 did not affect the mesogenic type and texture of $P1_2$. For P3 series, a diffuse peak at about $2\theta = 21°$ and a weak small-angle reflection at about $2\theta = 4.7°$ were observed, as shown in Figure 7(d). The result of X-ray diffraction analysis, POM, and optical rotation of the P3 indicated that P3 series is S_mC mesophase.

CONCLUSIONS

Three series of new main-chain LCPs P1, P2, and P3 series were prepared from sebacoyl chloride and various amount of 4,4′-biphenyldiol, isosorbide, and brilliant yellow. $P1_1$–$P1_6$ are S_mB^* and S_mC^* LCPs, which exhibited broken focal-conics texture and schlieren texture. $P1_0$, which does not contained isosorbide and BY, exhibited a typical smectic C texture. P3 series, which contained BY groups, are smectic C LCIs. P2 series are S_mB^* and S_mC^* LCIs containing both isosorbide and BY groups, which exhibited the broken focal-conics texture and schlieren texture. The introduction of ionic units in P2 will increase the thermal stability of the mesophase, but has not affected the mesogenic type and textures of LCP. Nevertheless, the introduction of chiral units in P2 leads to a change of mesophase, as compared with P3 series, which exhibited S_mC mesogetic phases.

References

1. Meyer, R. B. Mol Cryst Liq Cryst Sci Technol 1977, 40, 33.
2. Clark, N. A.; Lagerwall, S. T. Appl Phys Lett 1980, 36, 899.
3. Hans, R. K.; Nicolas, P.; Mihai, G.; Matthias, B. Macromolecules 1995, 28, 6565.
4. Aharoni, S. M. Macromolecules 1989, 22, 686.
5. Walba, D. M.; Keller, P.; Parmar, D. S.; Clark, N. A.; Wand, D. M. J Am Chem Soc 1989, 111, 8273.
6. Yuan, G.; Zhao, Y. Polymer 1995, 36, 2725.
7. Wiemesann, A.; Zentel, R. Polymer 1992, 33, 5315.
8. Zhao, Y.; Lei, H. Macromolecules 1994, 27, 4525.
9. Cochin, D.; Passmann, M. Macromolecules 1997, 30, 4775.
10. Wilbert, G.; Traud, S.; Zentel, R. Macromol Chem Phys 1997, 198, 3769.
11. Zhang, B. Y.; Weiss, R. A. J Polym Sci Part A: Polym Chem 1992, 30, 91.
12. Zhang, B. Y.; Weiss, R. A. J Polym Sci Part A: Polym Chem 1992, 30, 989.
13. Zhang, B. Y.; Guo, S. M.; Shao, B. J Appl Polym Sci 1998, 68, 1555.
14. Zhi, J. G.; Zhang, B. Y. J Appl Polym Sci 2001, 81, 2210.
15. Van't Hoff, J. H. Dielagerung der Atome im Raum, 2nd ed.; Vieweg & Sohn: Braunschweig, 1894; p 119.
16. Fitzgerald, J. J.; Weiss, R. A. J Macromol Sci Rev Macromol Chem Phys 1988, 28, 99.
17. Sato, M.; Kitani, Y. Liq Cryst 2003, 30, 9.